Corrigendum

Slit-mediated repulsion is a key regulator of motor axon pathfinding in the hindbrain

Rachel Hammond, Valerie Vivancos, Arifa Naeem, John Chilton, Elvira Mambetisaeva, William Andrews, Vasi Sundaresan and Sarah Guthrie *Development* **132**, 4483-4495.

The name of one of the authors is spelled incorrectly as Mambitisaeva in the printed and on-line versions of this article.

The correct spelling is Mambetisaeva.

The authors apologise for this mistake.

Slit-mediated repulsion is a key regulator of motor axon pathfinding in the hindbrain

Rachel Hammond, Valerie Vivancos, Arifa Naeem, John Chilton, Elvira Mambitisaeva, William Andrews, Vasi Sundaresan and Sarah Guthrie*

MRC Centre for Developmental Neurobiology, 4th Floor New Hunt's House, King's College, Guy's Campus, London SE1 1UL, UK
*Author for correspondence (e-mail: sarah.guthrie@kcl.ac.uk)

Accepted 11 August 2005

Development 132, 4483-4495
Published by The Company of Biologists 2005
doi:10.1242/dev.02038

Summary

The floor plate is known to be a source of repellent signals for cranial motor axons, preventing them from crossing the midline of the hindbrain. However, it is unknown which molecules mediate this effect in vivo. We show that Slit and Robo proteins are candidate motor axon guidance molecules, as Robo proteins are expressed by cranial motoneurons, and Slit proteins are expressed by the tissues that delimit motor axon trajectories, i.e. the floor plate and the rhombic lip. We present in vitro evidence showing that Slit1 and Slit2 proteins are selective inhibitors and repellents for dorsally projecting, but not for ventrally projecting, cranial motor axons. Analysis of mice deficient in *Slit* and *Robo* function shows that cranial motor axons aberrantly enter the midline, while ectopic expression of *Slit1* in chick embryos leads to specific motor axon projection errors. Expression of dominant-negative Robo receptors within cranial motoneurons in chick embryos strikingly perturbs their projections, causing some motor axons to enter the midline, and preventing dorsally projecting motor axons from exiting the hindbrain. These data suggest that Slit proteins play a key role in guiding dorsally projecting cranial motoneurons and in facilitating their neural tube exit.

Key words: Motoneurons, Hindbrain, Slit, Robo, Repulsion, Rat, Chick

Introduction

During development, axons are guided by contact-mediated and diffusible cues (Mueller, 1999; Huber et al., 2003). In the developing vertebrate embryo hindbrain, the floor plate is the origin of such cues, repelling motor axons and ensuring that they project ipsilaterally. Branchiomotor (BM) and visceral motor (VM) neurons differentiate in a ventral domain adjacent to the floor plate, while dorsally adjacent progenitors generate somatic motor (SM) neurons (Jessell, 2000; Vallstedt et al., 2001; Pattyn et al., 2003). SM neuronal somata remain ventrally, and their axons exit the neuroepithelium ventrally in small groups to innervate extraocular and tongue muscles. By contrast, BM and VM neurons translocate their somata dorsally and send their axons via large common dorsal exit points to innervate branchial arch and parasympathetic ganglion targets, respectively. Two neuronal subpopulations within r4 manifest other distinct migration behaviours. A subset of the small group of inner ear efferent (IEE) neurons translocate their somata across the midline (Fritzch and Nichols, 1993; Simon and Lumsden, 1993), while facial branchiomotor neuronal somata migrate caudally in some species (Auclair et al., 1996).

The floor plate produces repulsive signals (Guthrie and Pini, 1995), ensuring that motor axons and cell bodies do not cross the midline, and that BM/VM axons grow dorsally. Two molecules thought to mediate this effect are netrin 1 and semaphorin 3A (Sema3a), both of which repel BM/VM axons in collagen gel co-cultures, while only Sema3a repels the SM population (Colamarino and Tessier-Lavigne, 1995; Varela-Echavarría et al., 1997). However, there is no definitive evidence to suggest that netrin 1 or Sema3a operate in vivo to shape cranial motor axon pathways. Netrin 1 is expressed by the floor plate (Kennedy et al., 1994), but in netrin 1 mutants, no motor axon pathfinding defects have been reported (Serafini et al., 1996). No central defects in motoneuron projections have been reported in mice mutant for *Sema3a* or its receptor neuropilin 1 (Taniguchi et al., 1997; Kitsukawa et al., 1997). Moreover, Sema3a is not expressed by the hindbrain floor plate and therefore cannot account for the repulsive effects of this tissue in vitro (Varela-Echavarría et al., 1997; Chilton and Guthrie, 2003), although it is expressed by the mesenchyme underlying the hindbrain in the chick (Anderson et al., 2003) and in the mouse (V.V., M. Studer and S.G., unpublished). It therefore remains unknown whether additional chemorepellents are involved in motor axon repulsion.

We have therefore investigated the roles of the Slit guidance molecules and their Robo receptors in cranial motor axon guidance. In *Drosophila*, the Slit axon guidance molecules are important regulators of midline crossing (Kidd et al., 1999; Rajagopalan et al., 2000; Simpson et al., 2000), and in vertebrates Slit proteins are involved in the guidance of several groups of axons, including post-crossing commissural axons, cortical axons and retinal axons (Zou et al., 2000; Nguyen Ba-Charvet et al., 1999; Shu et al., 2002; Plump et al., 2002). Evidence that Slit2 repels spinal motor axons (SM) was

obtained in rodents (Brose et al., 1999), but the effects of Slit proteins on cranial motoneurons have not been tested.

In this paper, we show that expression patterns of Slit and Robo genes are consistent with their playing a role in cranial motor axon pathfinding. Using a well-established culture system for rat cranial motoneurons (see Caton et al., 2000), we find that Slit1 and Slit2 inhibit and repel the axons of dorsally projecting (BM/VM), but not ventrally projecting (SM), axons in vitro. Mice deficient in Robo or Slit gene function show axon navigation defects, with motor axons projecting aberrantly into or across the midline. In order to test the effects of focal overexpression of Slit proteins or of dominant-negative Robo receptors, we performed electroporation experiments in chick embryo hindbrains. Overexpression of *Slit* in chick hindbrains caused axon navigation errors, while BM/VM motor axons, which expressed dominant-negative Robo proteins, did not project away from the floor plate, and failed to exit the hindbrain correctly.

Materials and methods

In situ hybridisation and immunohistochemistry

In situ hybridisation for *Slit1*, *Slit2*, *Slit3*, *Robo1* and *Robo2* (probes were the kind gift of Dr M. Tessier-Lavigne) was performed on rat and chick embryos, some of which were previously retrogradely labelled with dextran axon tracers (Caton et al., 2000). Whole-mount in situ hybridisation was as previously described (Caton et al., 2000). Immunohistochemistry on paraffin sections was as described (Bancroft and Stevens, 1990) using anti-neurofilament antibodies and the S3 anti-Robo1/2 antibody (Sundaresan et al., 2004).

Collagen gel co-cultures

E12 rat embryo hindbrains were dissected into bilateral explants of the ventral third of the neuroepithelium, which contains motoneuron somata, and the floor-plate region, at the levels of rhombomere (r) 1, r2/3, r4/5, r6 and r7/8 (Naeem et al., 2002). Spinal cord explants were unilateral, and from thoracic levels. In some experiments motoneuron subpopulations were labelled before dissection using fluorescent axon tracers (Caton et al., 2000).

HEK293T cells were transfected with full-length human myc-tagged Slit expression constructs (hSlit1, hSlit2 or hSlit3; kind gift of Dr S. Sakano, Asahi Kasei Corporation) in pcDNA3.1 (Invitrogen) (Itoh et al., 1998) and made into clusters as described previously (Varela-Echavarría et al., 1997). Transfection was confirmed using antibody staining against Myc epitopes on the fusion proteins, while mock-transfected cells served as controls. Cell clusters were made in hanging drops and co-cultured with explants in collagen gels for 48 hours as previously described (Guthrie and Lumsden, 1994; Caton et al., 2000), in medium supplemented with heparin sulphate (50 ng/ml; Sigma, UK) (Brose et al., 1999; Hu, 2001). Immunohistochemistry on collagen co-cultures was performed using anti-neurofilament antibody for levels r2-8 (2H3, 1:100, DSHB, USA), or anti-SC1 antibody for trochlear r1 explants (F84.1, 1:20, kind gift of W. Stallcup) as described previously (Caton et al., 2000).

Assessment and quantitation of axon outgrowth in collagen gel co-cultures

All assessments of axon outgrowth were carried out blind. The response of F84.1-stained trochlear axons to the cell clusters was determined by measuring the angle between the lateral edge of the explant, and a line drawn down the centre of the fan of projecting trochlear axons (Scion Image programme) on both sides of the explant. In cases where the lateral explant edge was not straight, a line of best fit parallel to the floor plate was drawn. The 'angle difference' was calculated as the angle for the opposing side minus that for the facing side. Differences between data sets were evaluated using Student's *t*-test (two-tailed).

R2-8 explants were observed under phase contrast after 48 hours and semi-quantitative analysis was performed using a 0-5 index as described previously (Caton et al., 2000) where 0 indicates no axonal outgrowth and 5 indicates maximal axonal outgrowth. A net score (facing score – opposing score) was determined for each explant and statistical analysis of the data sets was performed using the Mann-Whitney U-test. Quantitative analysis (Scion Image programme) was carried out on neurofilament-stained explants, and involved counting the number of pixels surrounding each half of the explant. The number of pixels on the facing side was expressed as a percentage of the total number of pixels and results were tested statistically using the two-tailed *t*-test. For dextran-labelled explants, the number of axons facing towards the cell cluster was expressed as a percentage of the total number of labelled axons and group comparisons were performed using Student's *t*-test (two-tailed).

Analysis of Robo and Slit mutant mice

A Cre-flox strategy was used to generate a frame-shift mutation in the *Robo1* or *Robo2* gene, which induced a stop codon, and consequently led to mRNA decay and a 'null' phenotype. Exon 5 (an Ig domain) of *Robo1* or *Robo2* on a mouse BAC was floxed and used to generate a targeting vector (Southern or Western blot analyses were performed using standard techniques). ES cell cultures and generation of mice was carried out as previously described (Mombaerts et al., 1996). Founders were then mated with mice expressing Cre (under the actin promoter), yielding mice lacking the exon 5 cassette. Genotypes were assessed using PCR analysis – primers and conditions are available on request. Sequence analysis from E14 tissue samples confirmed the frame shift, and in situ hybridisation showed an absence of *Robo1* or *Robo2* mRNA in the spinal cord (data not shown). Absence of Robo1 or Robo2 protein was confirmed by western blot (data not shown). *Slit1* and *Slit2* mutant mice were a gift of Dr M. Tessier-Lavigne and have been described previously (see Plump et al., 2002; Bagri et al., 2002). In E11.5 embryos, dorsally projecting cranial motoneurons were labelled by injecting the lipophilic dye DiI into the cranial sensory ganglia [trigeminal, geniculate, petrosal and nodose to label respectively the trigeminal, (r2/r3) facial (r4/r5), glossopharyngeal (r6) and vagus (r7/8) motoneurons] as described previously (Guthrie and Lumsden, 1992). Briefly, hindbrain motor axons extend through, or in association with, these ganglia and therefore DiI injected into these regions labels the entire motoneuron via the membrane. As motoneurons are the only neurons with cell bodies within the hindbrain that extend axons via the ganglia, one can unequivocally say that motoneurons are labelled by this process (see Fig. 7E). Neurons and their entire axons are nicely shown by this labelling process, and therefore even when labelling multiple exit points simultaneously it is possible to clearly see whether motor axons from a particular axial level target to their correct exit point (e.g. whether r3 axons exit at r2; see Fig. 7D).

Electroporation of chick embryos in ovo

Hens' eggs were incubated to stage 10-11 and processed according to Momose et al. (Momose et al., 1999). The fourth ventricle was microinjected with the appropriate DNA construct: *hSlit1-myc* or *GFP*, truncated *Robo1Δ-GFP* or truncated *Robo2Δ-GFP* or myristylated *GFP*, each regulated by a β-actin promoter with a CMV enhancer. The truncated *Robo1Δ-GFP* and *Robo2Δ-GFP* transcripts consisted of the extracellular and transmembrane domain, but with the cytoplasmic domain deleted and a GFP tag substituted. Embryos were incubated to stages 17-19 and immunohistochemistry was performed as described previously (Guidato et al., 2003) using anti-SC1 (DSHB, USA; 1:10), anti-Myc (Autogen Bioclear, UK; 1:100), anti-islet1/2 (4D5, DSHB, USA; at 1:100) and anti-neurofilament H (1:600, Chemicon, UK).

Results

To discover whether Robo and Slit proteins are candidates to mediate cranial motor axon repulsion, we have used rodents and chicks, capitalising on the advantages of each. For example, culture experiments were carried out on rat embryo motoneurons, which show excellent growth in collagen gels, while global loss-of-function experiments were carried out using mutant mice, and local gain-of-function/loss-of-function experiments used electroporation in chick embryos. We first surveyed their expression patterns during the early stages of motoneuron development in the brainstem of rat embryos (Varela-Echavarría et al., 1997; Colamarino and Tessier-Lavigne, 1995; Varela-Echavarría et al., 1996). SM nuclei comprise the oculomotor nucleus in the midbrain, the trochlear nucleus in r1, the abducens nucleus in r5 and the hypoglossal nucleus in r8 (Fig. 1A). SM axons exit ventrally into the mesenchyme underlying the hindbrain, with the exception of trochlear SM axons, which extend dorsally within the midbrain-hindbrain boundary. Motor nuclei containing BM/VM neurons are the trigeminal nucleus in r2/3 (BM), the facial nucleus in r4/5 (BM/VM), the glossopharyngeal nucleus in r6 (BM/VM) and the vagus and cranial accessory nuclei in r7/8 (BM/VM and BM, respectively; Fig. 1A).

Slit proteins are expressed by the floor plate and the rhombic lip

In E11 and E12 rat embryos, we observed *Slit1* and *Slit2* expression within the floor plate at all axial levels (Fig. 1B,C; data not shown). Retrograde labelling of BM/VM or SM neurons in combination with in situ hybridisation for *Slit1* showed no expression by motoneurons (Fig. 1D,E). *Slit2* was also expressed throughout the floor plate, and in the caudal hindbrain (r5-8) in the regions of the differentiating SM neurons, as has been observed in the spinal cord (Fig. 1C) (Zou et al., 2000). *Slit2* (and to a lesser extent Slit1) was also expressed in the rhombic lip, which lies lateral to the motor exit points (Fig. 1B,C). In situ hybridisation for *Slit2* following retrograde dextran labelling of BM/VM cranial motoneurons clarified that there was no overlap (Fig. 1F), but retrograde labelling of SM neurons confirmed that they express *Slit2* (Fig. 1G). *Slit3* expression at E11 and E12 was similar to that of *Slit2*, but with no detectable expression in the rhombic lip, or in SM neurons (data not shown). In the chick embryo (stage 18), *Slit1* and *Slit2* were expressed in the floor plate, and *Slit2* was expressed in the rhombic lip, consistent with previous data (data not shown) (Gilthorpe et al., 2002).

Thus, Slit genes are expressed within the floor plate, consistent with a role in motor axon chemorepulsion from the midline, while *Slit2* expression in the rhombic lip might 'hem in' motor axon projections dorsally.

Robo proteins are expressed broadly in the neuroepithelium and by motoneurons

At E11, *Robo2* but not *Robo1* was expressed in columns corresponding with differentiating motoneurons (Fig. 1I; data not shown). At E12, *Robo1* and *Robo2* expression domains were similar, including the ventral half of the neuroepithelium and differentiating motoneurons (Fig. 1H,J). Axon tracing followed by in situ hybridisation and vibratome sectioning demonstrated that dorsally projecting BM/VM neurons and ventrally projecting SM neurons express *Robo1* and *Robo2* (Fig. 1K,L,M,N). In the chick hindbrain (stage 18), expression of *Robo1* and *Robo2* also encompassed the region of differentiating cranial motoneurons (data not shown).

Immunostaining using the S3 anti-Robo1/2 antibody (Sundaresan et al., 2004) and anti-neurofilament staining showed that both dorsally projecting motor axons (e.g. trigeminal) and ventrally projecting somatic motor axons (e.g. hypoglossal) express Robo proteins (Fig. 1O-R). Our expression data therefore demonstrate that at the mRNA level nascent motoneurons express *Robo2* at E11 and then both *Robo1* and *2* at E12, while Robo1 and/or Robo2 proteins are expressed by SM and BM/VM populations at E12. These expression patterns are consistent with the idea that Robo proteins (and in particular Robo2 at early stages) might transduce a Slit signal that drives motor axons away from the floor plate and later limits their trajectories dorsally.

Slit1 and Slit2 repel cranial motor axons in vitro

Collagen gel co-cultures were used to investigate the responses of cranial motoneurons (in bilateral E12 rat hindbrain explants) to cell clusters secreting Slit1-Slit3 (Fig. 2A). Previous studies have shown that these explants contain a high proportion of motoneurons, which project from the lateral sides of the explant (Guthrie and Pini, 1995; Varela-Echavarría et al., 1997; Caton et al., 2000). Explants were dissected from axial levels containing the trochlear nucleus (r1), trigeminal nucleus (r2/3), facial and abducens nuclei (r4/5), glossopharyngeal nucleus (r6), vagus, and cranial accessory and hypoglossal nuclei (r7/8) (Fig. 2A, compare with Fig. 1A). These were grown in collagen gels with their lateral sides 400-500 μm away from clustered cells that had been transiently transfected with *Slit1*, *Slit2* or *Slit3*, or mock-transfected as controls. Following 48 hours incubation, r2-8 explants were immunostained using anti-neurofilament antibodies, while those from r1 (trochlear) levels were immunostained using the anti-F84.1 antibody.

Semi-quantitative assessment of outgrowth from r2-8 explants was made under phase contrast, scoring each explant quadrant on a 0-5 index (see Materials and methods). In the presence of Slit1 and Slit2-secreting cell clusters, explants showed a consistent tendency to extend more axons from the side facing away from the cluster, indicating inhibition of growth by Slit proteins (Fig. 2B,C). Explants cultured in apposition to mock-transfected cells showed no inhibition of outgrowth or slight inhibition (Fig. 2E). The degree of asymmetry was analysed by subtracting the outgrowth score away from the cluster from that towards the cluster and deriving a percentage of explants showing each net score (see Fig. 2F-M). Values for explants cultured with Slit1/2 cells were consistently shifted to the left for all axial levels (i.e. showing more inhibition) compared with the corresponding control group. This inhibition was statistically significant for all axial levels, and appeared to be more pronounced for cultures with Slit2 (Fig. 2; see legend for *P* values).

Further quantitation of axon outgrowth on separate batches of r2-8 immunostained explants was performed by counting pixels on the side facing towards and away from the cell cluster (see Materials and methods; Fig. 2D), and showed a significant level of outgrowth inhibition (Fig. 2D) by Slit1/2 for all axial levels. At the trigeminal (r2 and 3) level, this inhibition was particularly striking, as Slit1- and Slit-2-exposed explants had a mean of 31% and 27%, respectively, of outgrowth present on

the facing side, both of which resulted in a *P* value of less than 8×10^{-8} when compared with the control group (Fig. 2B,C,E). For explants from other axial levels, Slit1 and Slit2 inhibited outgrowth with a mean of 33-36% of pixels on the facing side, thus showing a significant difference compared with controls.

Slit3-secreting cells did not cause any inhibition of outgrowth at any axial level (data not shown). The expression constructs for all three Slit proteins differed only in their inserts, while transfection levels were similar for all three constructs (data not shown), and previous work using an identical transfection system and the same constructs showed that the protein yield from cells transfected with Slit3 was similar to that seen with Slit1 and Slit2 (Patel et al., 2001). Therefore, technical differences are unlikely to explain this

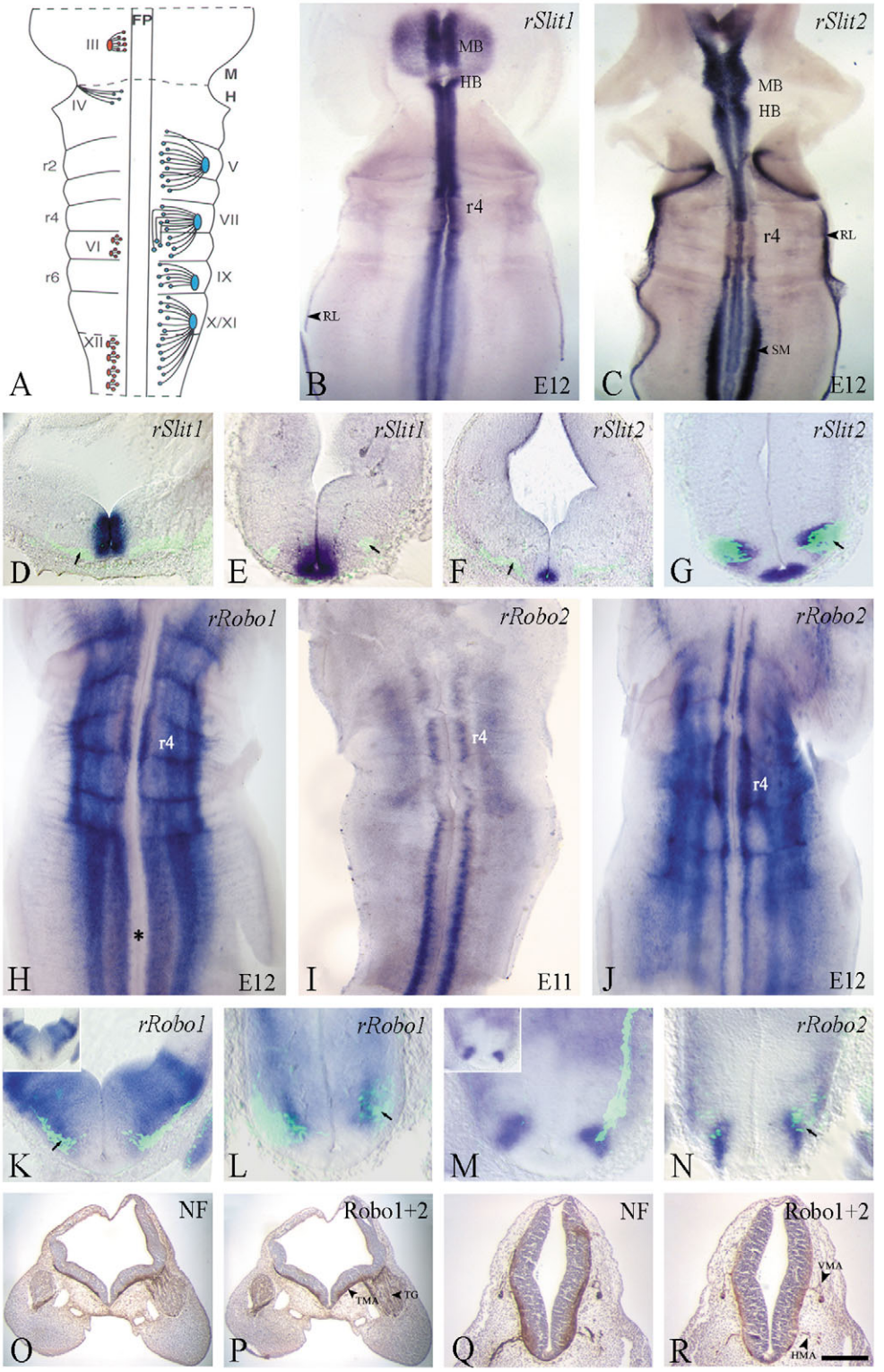

Fig. 1. Expression patterns of *Slit1* and *Slit2* and *Robo1* and *Robo2* in the rat embryo. (A) Diagram showing organisation of cranial motoneurons in E12 rat hindbrain; somatic motor (SM) neurons are on the left (red), BM/VM neurons are on the right (blue). Nuclei: III, oculomotor; IV, trochlear; V, trigeminal; VI, abducens; VII, facial; IX, glossopharyngeal; X/XI, vagus and cranial accessory; XII, hypoglossal (inner ear efferent neurons at r4 level omitted). (B,C,H-J) Flat-mount rat hindbrains in situ hybridised with *Slit* or *Robo* probes as indicated. Asterisk in H indicates the floor plate. (D-G,K-N) Vibratome sections of E12 rat embryos labelled with fluorescein dextran axon tracer then in situ hybridised; BM/VM projection labelled in D,F,K,M; SM projection labelled in E,G,L,N. Insets in K and M show in situ hybridisation without axon tracing. The axial levels of the vibratome sections are D rhombomere 2(r2); E, r5; F, r2; G, r8; K, r3; L, r7; M, r6; N, r6. (O-R) Peroxidase-stained sections of a rat E12 hindbrain with adjacent sections stained with neurofilament (NF) or anti-Robo1+2 antibodies as labelled. (O,P) r2/3 level; (Q,R) r8. HB or H, hindbrain; MB or M, midbrain; FP, floor plate; r, rhombomere; RL, rhombic lip; SM, somatic motoneurons; TMA, trigeminal motor axons; TG, trigeminal ganglion; VMA, vagus motor axons; HMA, hypoglossal motor axons. Scale bar: 500 μm in B,C,H,I,J,Q,R; 200 μm in D-G,K-N; 300 μm in O,P; 800 μm in insets.

result, pointing to a bona fide lack of response to Slit3.

Individual motoneuron subpopulations show differential responsiveness to Slit proteins

In r1 control explants, trochlear axons fanned out from the rostrolateral corners of the explant in a symmetrical pattern (Fig. 3G), while in the presence of Slit1- or Slit2-secreting cell clusters they were deflected rostrally, or in some cases projected towards the midline of the explant (Fig. 3A,D). The difference in the angle at which the bundle left each side of the explant was found to be symmetrical in the presence of mock-transfected cells, giving a mean difference in the projection angle of –3°. By contrast, in the presence of Slit1- or Slit2-expressing cell clusters, a mean angle difference of 17° or 18° respectively was detected, signifying a deflection of the bundle by Slit, and showing a significant difference from the control group (see Fig. 3B and legend).

Individual motoneuron subpopulations were also labelled via their dorsal (BM/VM) or ventral (SM) exit points using fluorescent dextran tracers, and the mean percentages of axons facing the cell cluster were quantitated. We found that for cultures with mock-transfected cells, BM/VM axons displayed symmetrical outgrowth, while Slit proteins inhibited BM/VM axon outgrowth from all axial levels (Fig. 3E,K,L,N,O). This represents significant inhibition, which was greatest for trigeminal levels (see Fig. 3 legend), consistent with the results obtained by quantitating total axon outgrowth from r2/3 explants. However, abducens (r5) and hypoglossal (r8) ventrally projecting SM neurons extended axons towards Slit-secreting cell clusters without impediment, showing equal outgrowth from towards and away-facing explant borders (Fig. 3H,J,M). Thus, ventrally projecting SM cranial motoneurons failed to respond to the Slit proteins.

We also performed co-cultures of SM spinal cord explants with Slit-secreting cells and observed radial outgrowth that was indistinguishable from that in the presence of mock-transfected cell clusters (Fig. 3C,F,H,I). This result is different from that

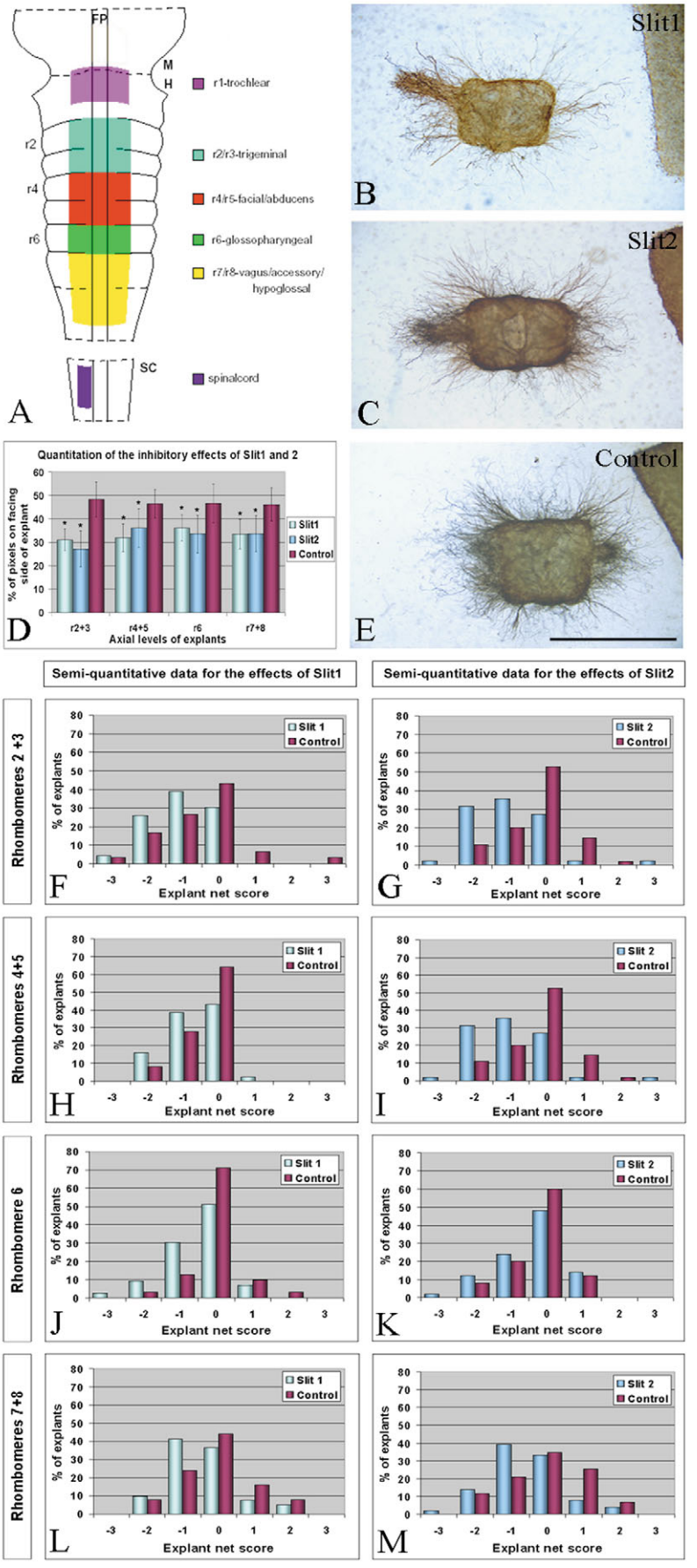

Fig. 2. Responses of motor axons to Slit proteins in vitro. (A) Dissection of tissues for use in collagen gel co-cultures (see Materials and methods). (B,C,E) Trigeminal (r2+3) level explants co-cultured with cells transfected as indicated. (D) Histogram showing quantitation (mean % pixels on facing side of explant are on the *y* axis) of outgrowth from explants at r2-8 levels in the presence of transfected cell clusters; $n>30$ for each condition. Asterisks represent significant differences from the controls. (F-M) Semi-quantitative data. A shift to negative explant net scores indicates inhibition of outgrowth (see Materials and methods); inhibition was significant when $P<0.1$ in all cases, and significant when $P<0.05$ in G,H,I,K,M; $n>25$ for each condition. Scale bar: 400 μm.

obtained by (Brose et al., 1999), who showed inhibition of spinal SM axon outgrowth by Slit. Taken together, our results show that Slit1 and Slit2 inhibit and repel cranial BM/VM axons, but not cranial or spinal SM axons. Trochlear axons project dorsally, despite being classified as SM subclass, and in our assays behave more like BM/VM axons (i.e. show repulsion). Of course, this result does not preclude a role for Slit/Robo proteins in other aspects of SM neuronal development, while a possible role in axon pathfinding of the oculomotor nerve (not tested here) remains possible.

Cranial motor axons show pathfinding errors in Robo and Slit mutant mice

In order to evaluate the in vivo importance of Robo-Slit signalling, we investigated the hindbrains of E11.5 mouse embryos mutant for *Robo1* or *Robo2* and *Slit1*/*Slit2*, using DiI labelling of BM/VM axon pathways. Analysis was restricted to the latter populations as our in vitro data suggested that SM neurons were unresponsive to Slit proteins. In wild-type embryos at this stage, all motoneuron cell bodies and axons lie ipsilateral to the floor plate, with the exception of r4 and rostral r5 level, where some processes and cell bodies of inner ear efferent (IEE) neurons (which may be, arguably, classified as motoneurons) cross the midline (Fig. 4A,B) (Fritzsch and Nichols, 1993; Simmons, 2002). Some facial BM neurons that originate in r4 are commencing their caudal migration through r5 towards r6 (Fig. 4A) (Auclair et al., 1993; Studer et al., 1996; Goddard et al., 1996).

Disruption of this pattern of axon projections was observed in mice deficient in Slit or Robo gene function. DiI labelling showed that there was no overall reduction in numbers of motoneurons relative to wild-type embryos, and that axons

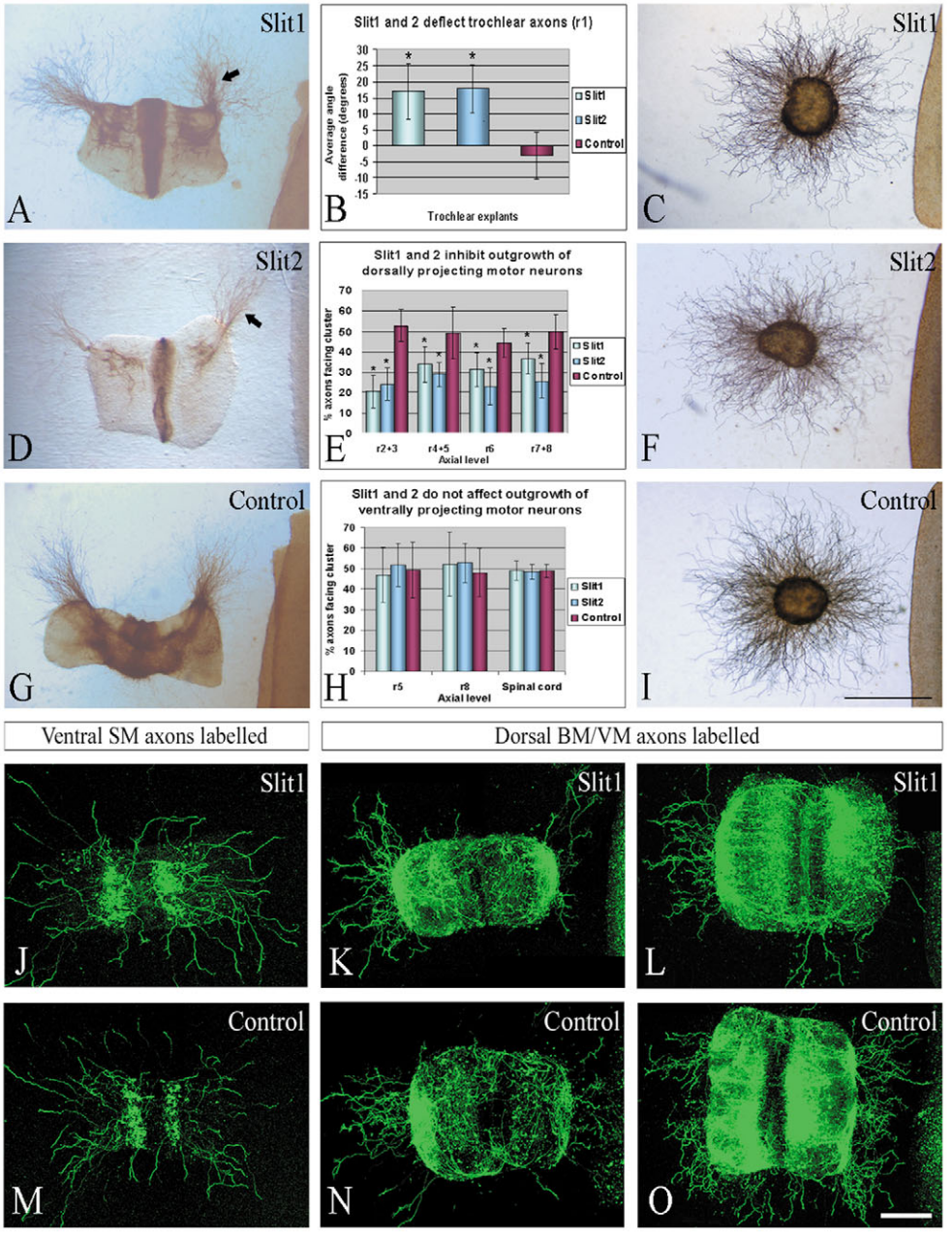

Fig. 3. Responsiveness of motoneuron subpopulations to Slit proteins in vitro. (A,D,G) Immunostained trochlear axons from explants co-cultured with transfected cell clusters. (B) Histogram showing mean angle difference representing trochlear axon bundle chemorepulsion. Significant differences from controls represented by asterisks (P<0.05); n>20 in each condition. (C,F,I) Spinal cord explants growing in the presence of transfected cell clusters. (E,H) Histograms representing quantitation of mean % of axons facing cluster (y-axis) for retrogradely labelled dorsally projecting (BM/VM) axons (E) or ventrally projecting (SM) axons (H). Asterisks indicate significant deviations from the control values (P<0.05); n>10 for BM/VM labelled explants, n>25 for SM labelled explants. (J-L) Explants placed in apposition to *Slit1*-transfected cell clusters. (M-O) Explants facing mock-transfected control cell clusters. (J,M) Ventrally projecting abducens axons. (K,N) Dorsally projecting glossopharyngeal axons. (L,O) Dorsally projecting hypoglossal/cranial accessory axons. Scale bars: 400 μm in I for A,C,D,F,G,I; 400 μm in O for J-O.

Table 1. Total number of axons displaying different behaviours for each genotype

Axial level (r=rhombomere)	Axonal behaviours	*Slit1*$^{-/-}$; *Slit2*$^{-/-}$	*Robo1*$^{+/-}$; *Robo2*$^{+/-}$	*Robo1*$^{-/-}$; *Robo2*$^{+/+}$	*Robo1*$^{+/+}$;*Robo2*$^{-/-}$	Wild type
r2+r3	Number crossing between fascicles*	i.d.	0	2	2	0
	Number crossing the floor plate	i.d.	8	6	7	0
	Number longitudinally projecting axons in the floor plate	i.d.	0	0	0	0
r4+r5	Number crossing between fascicles*	0	12	20	12	4
	Number crossing the floor plate	49	91	81	193	100
	Number longitudinally projecting axons in the floor plate	9	25	17	61	0
r6	Number crossing between fascicles*	i.d.	i.d.	0	0	0
	Number crossing the floor plate	i.d.	i.d.	8	3	0
	Number longitudinally projecting axons in the floor plate	i.d.	i.d.	0	0	0
Number of embryos		*n*=3	*n*=6	*n*=8	*n*=7	*n*=11

i.d., insufficient data.
*Bundles of axons en route to the exit point.

targeted normally to their exit points. Cranial motor axon pathways in *Slit1*$^{-/-}$ mutants resembled those in wild-type animals, as previously reported for other projections (Plump et al., 2002; Long et al., 2004). However, defects were detected in *Slit1*$^{-/-}$;*Slit2*$^{-/-}$ animals, in which axons within r4/5 failed to cross the floor plate directly, and instead projected for short distances longitudinally between fascicles (Fig. 4C), or entered the floor plate and failed to exit (Fig. 4D). Similar defects were observed in *Robo1/2* double heterozygotes (data not shown). In *Robo1*$^{-/-}$ or *Robo2*$^{-/-}$ mutants, more severe defects were observed, and while the projection pattern viewed at low power was grossly normal (Fig. 4G), at r4/5 levels axons entered the midline and projected rostrally and caudally within the floor plate, forming long fascicles (Fig. 4E,F). Defects of motor axon pathfinding also occurred at other axial levels. Within r2/3, some trigeminal axons projected longitudinally between fascicles, rather than growing laterally towards their exit point (Fig. 4H), and at r2/3 and r6 levels, axons crossed or looped back across the midline (Fig. 4I,J). Ectopic projections were quantitated in a subset of embryos of each genotype (Table 1). For *Slit1/2* mutants, *Robo1/2* double heterozygotes and *Robo1* mutants, the numbers of axons crossing the floor plate at r4/5 level were similar to those in wild-type embryos. However, for Robo2 mutants these numbers were strongly increased. As IEE

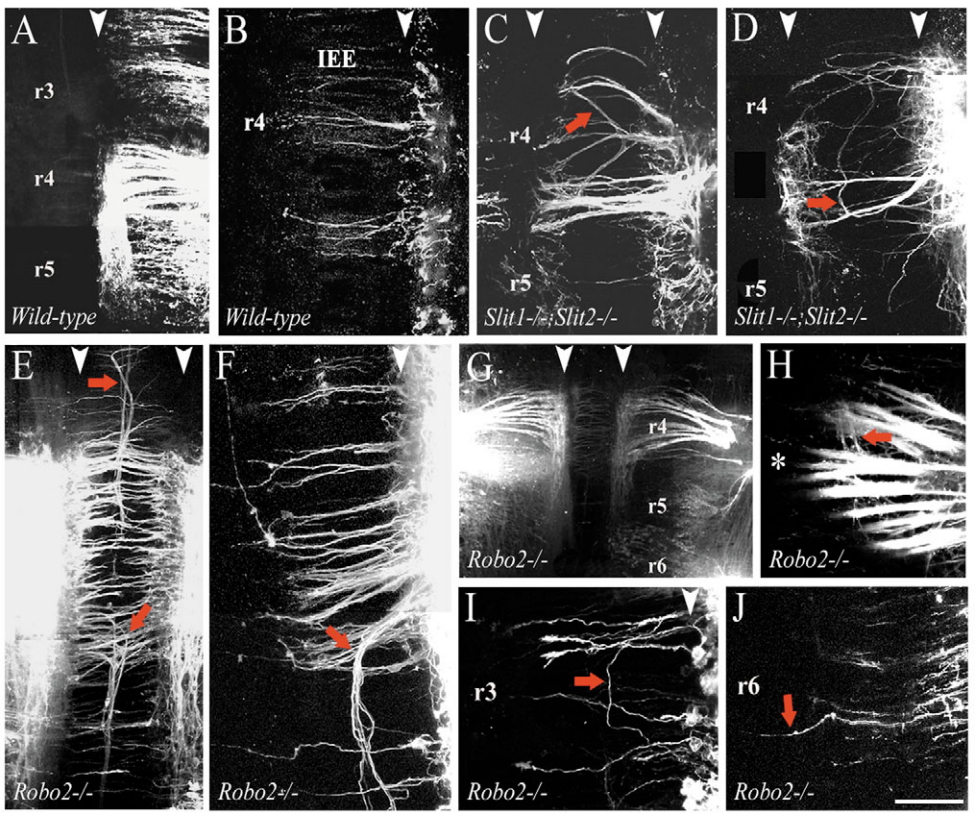

Fig. 4. DiI labelling of motor axon pathways in the hindbrains of E11.5 mouse embryos mutant for Slit proteins or Robo proteins. All panels show flat-mount hindbrains with DiI labelling of dorsally projecting BM/VM neurons. (A,E) DiI labelling is bilateral; (B-D,F-H) labelling is unilateral (right-hand side). Genotypes as labelled. Rhombomeres are numbered, white arrowheads indicate floor-plate borders and red arrows indicate axon guidance errors. (A,B,F,I) Floor plate is to left of the white arrow. (H) Basal plate with floor plate towards the left (asterisk). (J) Centre of floor plate. IEE, inner ear efferent axons. Scale bar: 200 μm in A,G; 400 μm in B-F,H.

axons normally cross the floor plate at r4/5, excessive crossing is likely to represent facial BM axons. In addition, axons were seen projecting longitudinally within the floor plate in all genotypes, with the greatest numbers seen in *Robo2* mutants. Embryos in which BM or IEE neurons only were labelled showed longitudinal axon fascicles, suggesting that both populations exhibit this behaviour.

Further analysis of the mutant mice by double immunostaining cryosections with anti-Islet 1/2 and anti-neurofilaments antibodies failed to reveal significant numbers of motoneuron cell bodies within the floor plate, suggesting that cell body position was normal, and was not affected by attenuation of Slit-Robo signalling (data not shown). Anti-neurofilament immunostaining of whole-mount E11.5 embryos did not show abnormalities of peripheral motor axon pathways. This implies that the major role of Slit-mediated interactions on cranial motor axons is within the neural tube.

Electroporation of Slit or dominant-negative Robo proteins in vivo causes motor axon pathfinding errors

We next tested the effects of overexpression of *Slit1*, or of dominant-negative *Robo1* or *Robo2* expression plasmids in chick hindbrains in ovo. These plasmids were electroporated into chick embryos at stages 10-11, and embryos were harvested at HH stage17-19 to examine motor axon pathways. A *Slit1-Myc* construct was used, or *GFP* as a control, and anti-SC1 antibodies were used to detect early motor axon projections (Simon et al., 1994).

In control GFP electroporations, axons projected normally at all axial levels on both the electroporated and non-electroporated sides of the embryo; at r3 and r5 levels axons curved rostrally towards their exit points in r2 and r4, respectively (Fig. 5A). By contrast, motor axons showed misprojections within the *Slit1-Myc*-expressing region. At r3 and r5 levels, some axons projected caudally to the r4 or r6 exit point, respectively, rather to their correct, rostral exit point (Fig. 5B-D; n=12/12 for r3; n=12/16 for r5). At r6 level, glossopharyngeal motor axons displayed distinct misprojections within the region of ectopic *Slit1-Myc* expression, overshooting their dorsal exit point, and forming tangles (Fig. 5E,F; n=14/14). These phenomena was also observed at r7/8 levels (n=4/4; data not shown). At all axial levels, axon stalling was also frequently observed within the *Slit-Myc* expressing domain (Fig. 5D; n=14/20), with axons failing to reach their exit points; this suggests that motor axon growth is inhibited in response to ectopic Slit protein in vivo.

We next electroporated constructs encoding truncated Robo1 or Robo2 proteins, which contained the extracellular domain and transmembrane domain, with a GFP tag in place of the deleted cytoplasmic domain – *Robo1Δ-GFP* or *Robo2Δ-GFP*. Robo proteins truncated in this manner fail to transduce a signal, and such constructs have previously been used to reduce or abrogate Slit-Robo signalling (Stein and Tessier-Lavigne, 2001; Whitford et al., 2002). Electroporated motoneurons were identified by immunostaining for Islet1/2 and their GFP-labelled axons. In control embryos electroporated with a myristylated form of GFP (which is targeted to the membrane), *GFP*-expressing neurons showed normal axon projections with no motor axons or cell bodies within the floor plate (Fig. 6A).

By contrast, chick hindbrains electroporated with either the *Robo1Δ-GFP* or the *Robo2Δ-GFP* constructs showed dramatic axon guidance defects in the BM/VM axon pathways. Anti-neurofilament immunostaining confirmed that these defects were not due to global effects on hindbrain axon pathways (Fig. 6F). The majority of *Robo1Δ-GFP*-expressing motor axons failed to project away from the midline, and instead stalled or projected parallel to the floor plate (Fig. 6B,C). Axons that did project dorsally had wandering or looping trajectories, and very few *Robo1Δ-GFP*-expressing motor axons reached their dorsal exit points (<20 in n=5 embryos at r2/3 level; <15 in n=7 embryos at r4/5 level; 0 in n=7 embryos at r6 level). Embryos containing *Robo2Δ-GFP*-electroporated motor axons showed very similar defects to those described above (Fig. 6D-F; n=19/19 cases).

When electroporated hindbrains were viewed at higher magnification, myr-GFP labelled axons extended away from the floor plate (Fig. 6J), except at r4/5 axial level, where floor plate-crossing axons of IEE neurons were found. Analysis of embryos expressing dominant-negative Robo proteins showed that electroporated motoneurons resided in the floor plate at many levels other than r4/5, and their GFP-labelled axons often behaved abnormally. Many axons extended into the floor plate and either grew longitudinally, crossed to the other side, or looped

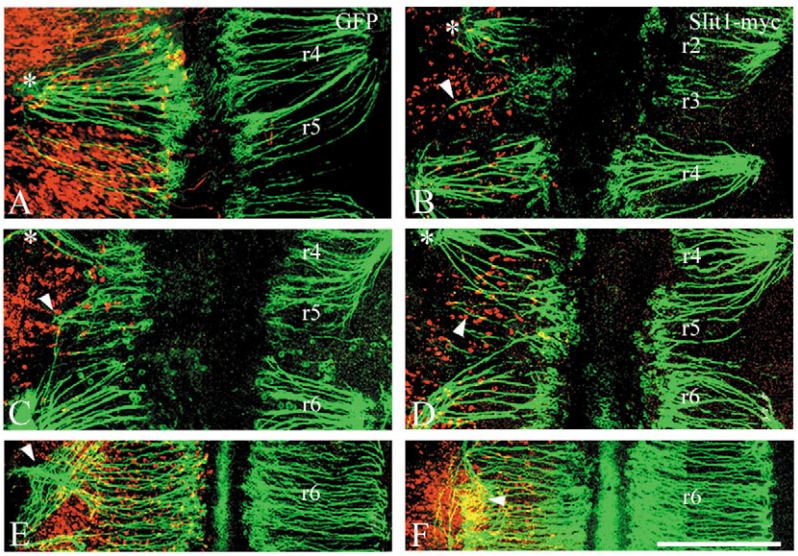

Fig. 5. Effects of ectopic expression of Slit1 in chick hindbrains. All panels show flat-mount chick hindbrains electroporated at stage 10-11, fixed at stage 17-19 and immunostained using anti-SC1 antibodies to show motor axon pathways (green). (A) A control GFP construct has been electroporated (red); (B-F) a *hSlit1-myc* construct has been electroporated (red). Rhombomere levels are numbered on the non-electroporated (right-hand) side. Exit points are shown by an asterisk in some cases. White arrowheads show regions in which axons exit at the incorrect exit point (B,C), stall (D) or overshoot the exit point and form tangles (E,F). Scale bar: 150 μm.

back to the side of origin (*Robo1Δ-GFP* 31 axons in 9 embryos; *Robo2Δ-GFP* 14 axons in 8 embryos; Fig. 6G-J). These data suggest that *Robo1Δ-GFP*-expressing neurons/axons do not respond to repellent guidance cues found at the midline.

To determine whether electroporated BM/VM axons were able to traverse their exit points into the periphery, we immunostained transverse cryosections of electroporated hindbrains with anti-Islet1/2 and anti-neurofilament antibodies. In these sections, axons expressing *myr-GFP* could be observed projecting from both ventral (SM) and dorsal (BM/VM) exit points into the periphery (Fig. 6L). By contrast, *Robo1Δ-GFP* and *Robo2Δ-GFP*-expressing axons projected via ventral and not dorsal exit points (Fig. 6K,M,N; insets). A small proportion of *Robo1Δ-GFP* and *Robo2Δ-GFP*-expressing motor axons were seen to project dorsally (as in the flat-mounted preparations) but did not traverse the exit point. The most likely interpretation of these results is that a lack of Slit-Robo signalling not only hampers the ability of motor axons to pursue an initial trajectory away from the midline, but also impairs their ability to locate and traverse the dorsal exit points.

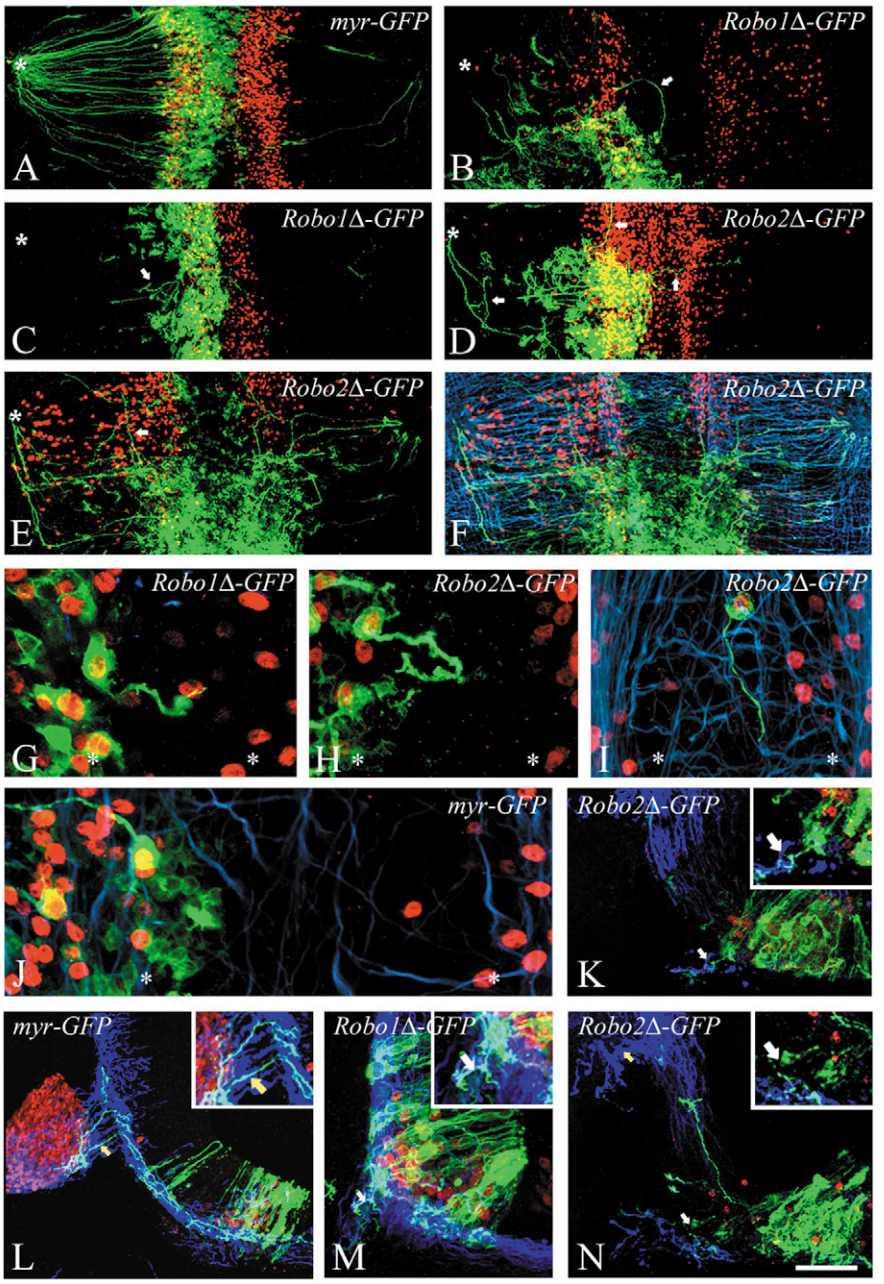

Fig. 6. Effects of expression of dominant-negative Robo1 and Robo2 constructs in chick hindbrains. (A-J) Flat-mount chick hindbrains that have been electroporated with plasmids encoding myristylated GFP (*myr-GFP*), dominant-negative Robo1-GFP (*Robo1Δ-GFP*) or Robo2-GFP (*Robo2Δ-GFP*) as labelled. Hindbrains were fixed at stage 17-19 and immunostained with anti-Islet 1/2 antibodies to detect motoneuron cell bodies (red), while GFP expression is shown in green. (F,I-N) Preparations additionally immunostained using anti-neurofilament antibodies (blue) to reveal all axon tracts. (G-J) Asterisks show borders of floor plate. (K-M) Transverse cryostat sections of embryos electroporated with plasmids labelled as above, with insets showing higher magnification. Immunostaining is as above. Yellow and white arrows show dorsal and ventral exit points, respectively. Both dorsal and ventral GFP-labelled motor axons exit in the control whereas only ventral axon projections are present in the dominant-negative Robo-electroporated embryos. (L) The trigeminal ganglion is immunostained in red (Islet 1/2). Scale bar: 100 μm in A-F; 15 μm in G-I; 50 μm in K,L,N; 30 μm in M; 20 μm in insets.

Discussion

In this study we have shown that Slit-Robo signalling is likely to play a key role in cranial motor axon navigation in vivo. In vitro assays showed that Slit1 and Slit2, but not Slit3, inhibit and repel the dorsally projecting axons of BM/VM hindbrain neurons. By contrast, Slit proteins do not repel ventrally projecting cranial and spinal SM axons. Ectopic expression of Slit1 in chick hindbrains caused axons to misproject, stall and overshoot their exit points. Attenuation of Slit-Robo signalling in either chick or mouse embryos resulted in BM/VM motor axons aberrantly entering the ventral midline, and failing to project dorsally or to reach their exit points. Slit proteins secreted by the midline floor plate thus appear to repel BM/VM motor axons, directing them dorsally, while Slit proteins present at the rhombic lip may circumscribe their pathways dorsally (schematised in Fig. 7).

Expression, in vitro and in vivo studies are consistent with a repellent role for Slit

This study has demonstrated that *Slit1* and *Slit2* are expressed by the floor plate and the rhombic lip, consistent with previous studies (E9.5-E11.5) (Brose et al., 1999; Holmes et al., 1998; Yuan et al., 1999; Zou et al., 2000; Gilthorpe et al., 2002). Our

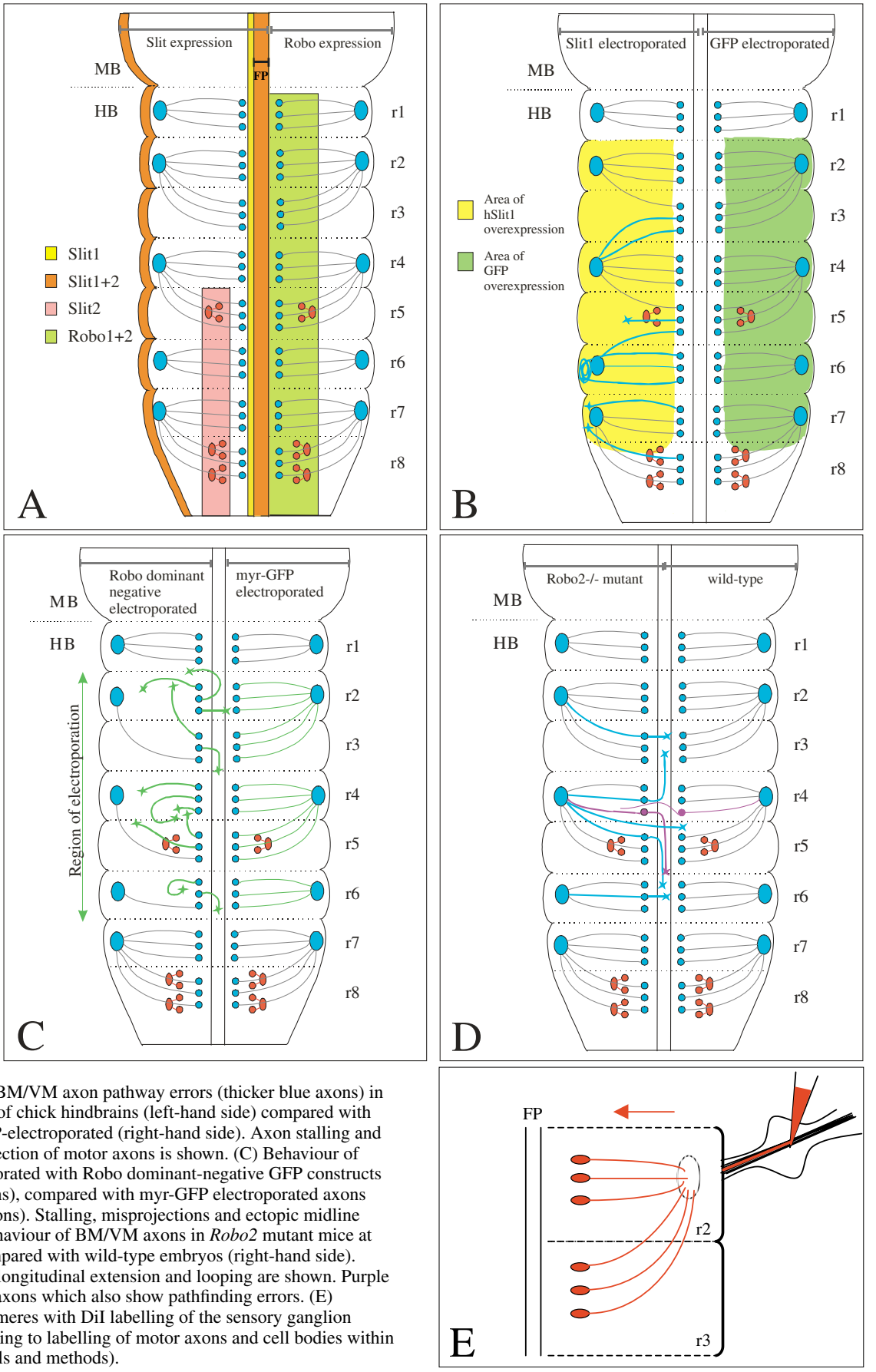

Fig. 7. The role of Slit-Robo signalling in motor axon pathfinding in the hindbrain. (A-D) Schematic diagrams of the vertebrate embryo hindbrain at stage 19 chick (A-C) or E11.5 mouse (D) is presented. Rhombomere levels are indicated (r) and the midbrain (MB)-hindbrain (HB) boundary. BM/VM neurons are shown in blue with corresponding exit points (blue ellipses) while SM neurons are shown in red. (A) Composite patterns of Slit and Robo expression (see key) in regions relevant to this study. (B) BM/VM axon pathway errors (thicker blue axons) in Slit1-electroporated sides of chick hindbrains (left-hand side) compared with non-electroporated or GFP-electroporated (right-hand side). Axon stalling and inappropriate, caudal projection of motor axons is shown. (C) Behaviour of BM/VM neurons electroporated with Robo dominant-negative GFP constructs (left-hand side; green axons), compared with myr-GFP electroporated axons (right-hand side; green axons). Stalling, misprojections and ectopic midline crossing is shown. (D) Behaviour of BM/VM axons in *Robo2* mutant mice at E11.5 (left-hand side) compared with wild-type embryos (right-hand side). Ectopic midline crossing, longitudinal extension and looping are shown. Purple axons in D represent IEE axons which also show pathfinding errors. (E) Schematic of two rhombomeres with DiI labelling of the sensory ganglion outside the hindbrain, leading to labelling of motor axons and cell bodies within the hindbrain (see Materials and methods).

study is the first to show that cranial motor populations express *Robo1* and *Robo2* at early stages in the rat (Fig. 7A).

The proposed role of Slit proteins as a stop signal from the rhombic lip is consistent with our previous demonstration that the roof plate and alar plate of the rat hindbrain repels cranial motor axons (Caton et al., 2000), and with suggestions that Slit proteins often act to form repulsive corridors (Erskine et al., 2000; Bagri et al., 2002). The in vitro repulsion of BM/VM neurons by Slit1 and Slit2 supports this idea; trigeminal axons exhibited the strongest responses to Slit proteins, consistent with the prominent expression of Robo proteins within r2/3 levels. Overexpression of Slit in the chick hindbrain caused BM/VM axon misprojections to the incorrect exit point, stalling and overshooting (Fig. 7B). Axon overshooting suggests that the rhombic lip expression of Slit normally limits axon extension dorsally, with uniform Slit expression rendering axons unable to distinguish this dorsal boundary, while stalling is presumably a 'growth cone collapse' type response. Projections to the incorrect exit point by axons in odd-numbered rhombomeres (r3 and r5) imply that these axons are more sensitive to Slit, and that local repulsion causes them seek out the nearest exit point. An alternative explanation, however, is that overexposure to Slit ligands modifies the abilities of motor axons to respond to specific exit-point derived signals, which as yet remain uncharacterised (Guthrie and Lumsden, 1992; Warrilow and Guthrie, 1999).

BM/VM cranial motor axons fail to exit the midline or the hindbrain when Slit-Robo signalling is attenuated

Experiments in which Slit-Robo signalling was attenuated either in mouse mutants or using dominant-negative approaches in the chick showed strikingly similar phenotypes. In *Slit1/2* double mutants, signalling via Slit3 would be expected to occur (although our in vitro experiments in the rat suggest that Slit3 is not repulsive), whereas we were unable to generate *Robo1/2* double mutants. Thus, we did not assess motor axon projections in mice in the complete absence of Slit-Robo signalling. However, attenuating this signalling might be expected to result in a randomisation of axon projections with a loss of projections away from the midline. The most striking phenotypes were seen in *Robo2* mutants, suggesting that *Robo2* may be the crucial receptor for cranial motor axon guidance in rodents, consistent with our observation in rat embryos of an earlier onset of expression of *Robo2* in hindbrain motoneurons (Fig. 7D). It is interesting that motor axon phenotypes observed at r4/5 levels were similar to those seen in *Ephb2*$^{-/-}$ mice and *Gata3*$^{+/-}$ mice; in both cases, aberrant longitudinal motor axons in the floor plate were attributed to IEE projections (Cowan et al., 2000; Karis et al., 2001). This raises the possibility that *Gata3* might regulate levels of Robo proteins and Eph receptors required for midline exit by IEE axons. Our favoured interpretation is that both facial BM and IEE axons projected longitudinally in *Robo2* mutants, while aberrant midline crossing by BM/VM axons occurred at all axial levels, but particularly r4/5.

The most striking effect of reducing Slit-Robo signalling in chicks was to disrupt BM/VM axon projections away from the midline and prevent them from exiting the neural tube (Fig. 7C). Therefore, Slit signalling seems to polarise motoneurons, allowing them to extend only one laterally orientated axon. The failure of BM/VM axons expressing the dominant-negative receptor to reach the periphery might imply that cranial motoneurons require early and transient Slit-Robo signalling in order to later manifest sensitivity to other cues, such as exit point-derived signals or HGF (Guthrie and Lumsden, 1992; Caton et al., 2000; Naeem et al., 2002). Transient Slit exposure might constitute part of a switch that changes motor axon growth from a repulsive mode (away from the midline) to an attractant one (towards the periphery).

Which are the chemorepellents for BM/VM and SM axons in vivo?

In vitro assays revealed a differential effect of Slit proteins on cranial motoneuron subpopulations, with strong repulsion by Slit1 and Slit2 of BM/VM axons, but not SM axons. Another study has reported repulsion of spinal motor axons (though not of cranial SM axons) by Slit2 (Brose et al., 1999), and the reasons for the discrepancy is unclear, but may be technical. Interestingly, Patel et al. (Patel et al., 2001) showed that addition of Robo1-Fc to co-cultures of spinal motor explants and floor-plate tissue did not block floor-plate-mediated repulsion, thereby suggesting that Slit proteins were not involved in this process. As SM neurons of the caudal hindbrain themselves express Slit2 at early stages of development, it is possible that the endogenous Slit2 expression desensitises SM axons to exogenous ligands, as has been shown for ephrin A proteins (Hornberger et al., 1999). The expression of Slit2 by this motoneuron population might also affect its ability to respond to netrin 1, as Slit2 has been shown to bind netrin 1 (Brose et al., 1999) and SM neurons do not respond to netrin 1 in vitro (Varela-Echavarría et al., 1997), despite expressing the Unc5h1 receptor (Barrett and Guthrie, 2001).

Thus, cranial SM neurons do not respond to either netrin 1 or Slit proteins; as SM axons exit the hindbrain ventrally and then project rostrally or caudally in mesenchyme on either side of the notochord and close to the midline, a lack of responsiveness to midline repellents might be a prerequisite of the pathway. Only Sema3a has thus far been identified as a chemorepellent for cranial SM neurons, and this ligand is not expressed by the hindbrain floor plate, leaving undetermined which floor-plate-secreted repellent prevents SM axons from crossing the midline (Guthrie and Pini, 1995). Sema3a expression by the notochord (Anderson et al., 2003) might dictate the position of the longitudinal tracts within the mesenchyme.

Here, we have provided in vivo evidence that Slit-Robo signalling is involved in cranial motor axons repulsion from the midline; currently evidence of an in vivo role for netrin 1 and Sema3a in this process is lacking. The relative contribution of different repellent mechanisms remains to be evaluated.

We thank Dr S. Sakano and Asahi Kasei Corporation for the provision of Slit expression plasmids, and Dr W. Stallcup for F84.1 antibody. We also thank Carl Hobbs for performing paraffin wax sectioning and immunohistochemistry, and Drs U. Drescher and R. Wingate for valuable discussions on the manuscript.

References

Anderson, C. N., Ohta, K., Quick, M. M., Fleming, A., Keynes, R. and Tannahill, D. (2003). Molecular analysis of axon repulsion by the notochord. *Development* **130**, 1123-1133.

Auclair, F., Valdes, N. and Marchand, R. (1996). Rhombomere-specific origin of branchial and visceral motoneurones of the facial nerve in the rat embryo. *J. Comp. Neurol.* **369**, 451-461.

Bagri, A., Marin, O., Plump, A. S., Mak, J., Pleasure, S. J., Rubenstein, J. L. and Tessier-Lavigne, M. (2002). Slit proteins prevent midline crossing and determine the dorsoventral position of major axonal pathways in the mammalian forebrain. *Neuron* **33**, 233-248.

Bancroft, J. D. and Stevens, A. (1990). *Theory and Practice of Histological Techniques*. 3rd edn. London: Churchill Livingstone.

Barrett, C. and Guthrie, S. (2001). Expression patterns of the netrin receptor UNC5H1 among developing motor neurons in the embryonic rat hindbrain. *Mech. Dev.* **106**, 163-166.

Brose, K., Bland, K. S., Wang, K. H., Arnott, D., Henzel, W., Goodman, C. S., Tessier-Lavigne, M. and Kidd, T. (1999). Slit proteins bind Robo receptors and have an evolutionarily conserved role in repulsive axon guidance. *Cell* **96**, 795-806.

Caton, A., Hacker, A., Naeem, A., Livet, J., Maina, F., Bladt, F., Klein, R., Birchmeier, C. and Guthrie, S. (2000). The branchial arches and HGF are growth-promoting and chemoattractant for cranial motor axons. *Development* **127**, 1751-1766.

Chilton, J. and Guthrie, S. (2003). Cranial expression of class 3 secreted semaphorins. *Dev. Dyn.* **228**, 726-733.

Colamarino, S. and Tessier-Lavigne, M. (1995). The axonal chemoattractant netrin-1 is also a chemorepellent for trochlear motor axons. *Cell* **81**, 621-629.

Cowan, C. A., Yokoyama, M., Bianchi, L. M., Henkemeyer, M. and Frizsch, B. (2000). EphB2 guides axons at the midline and is necessary for normal vestibular function. *Neuron* **26**, 417-430.

Erskine, L., Williams, S. E., Brise, K., Kidd, T., Rachel, R. A., Goodman, C. S., Tessier-Lavigne, M. and Mason, C. A. (2000). Retinal ganglion cell axon guidance in the mouse optic chiasm: expression and function of robos and slits. *J. Neurosci.* **20**, 4975-4982.

Fritzsch, B. and Nichols, D. H. (1993). DiI reveals a prenatal arrival of efferents at the differentiating otocyst of mice. *Hear. Res.* **65**, 51-60.

Gilthorpe, J. D., Papantoniou, E.-K., Chedotal, A., Lumsden, A. and Wingate, R. J. T. (2002). The migration of cerebellar rhombic lip derivatives. *Development* **129**, 4719-4728.

Goddard, J. M., Rossel, M., Manley, N. R. and Capecchi, M. R. (1996). Mice with targeted disruption of Hoxb-1 fail to form the motor nucleus of the VIIth nerve. *Development* **122**, 3217-3228.

Guidato, S., Prin, F. and Guthrie, S. (2003). Somatic motor neurone specification in the hindbrain: the influence of somite-derived signals, retinoic acid and Hoxa3. *Development* **130**, 2981-2996.

Guthrie, S. and Lumsden, A. (1992). Motor neuron pathfinding following rhombomere reversals in the chick embryo hindbrain. *Development* **114**, 663-673.

Guthrie, S. and Lumsden, A. (1994). Collagen gel coculture of neural tissue. *Neuroprotocols* **4**, 116-120.

Guthrie, S. and Pini, A. (1995). Chemorepulsion of developing motor axons by the floor plate. *Neuron* **14**, 1117-1130.

Holmes, G. P., Negus, K., Burridge, L., Raman, S., Algar, E., Yamada, T. and Little, M. H. (1998). Distinct but overlapping expression patterns of two vertebrate slit homologues implies functional roles in CNS development and organogenesis. *Mech. Dev.* **79**, 57-72.

Hornberger, M. R., Dutting, D., Ciossek, T., Yamada, T., Handwerker, C., Lang, S., Weth, F., Huf, J., Wessel, R., Logan, C. et al. (1999). Moldulation of EphA receptor function by coexpressed ephrinA ligands on retinal ganglion cell axons. *Neuron* **22**, 731-742.

Hu, H. (2001). Cell-surface heparan sulfate is involved in the repulsive guidance activities of Slit2 protein. *Nat. Neurosci.* **4**, 695-701.

Huber, A. B., Kolodkin, A. L., Ginty, D. D. and Cloutier, J.-F. (2003). Signalling at the growth cone: ligand-receptor complexes and the control of axon growth and guidance. *Annu. Rev. Neurosci.* **26**, 509-563.

Itoh, A., Miyabayashi, T., Ohno, M. and Sakano, S. (1998). Cloning and expression of three mammalian homologues of Drosophila slit suggest possible roles for Slit in the formation and maintenance of the nervous system. *Brain Res. Mol. Brain Res.* **62**, 175-186.

Jessell, T. M. (2000). Neuronal specification in the spinal cord: inductive signals and transcriptional codes. *Nat. Genet.* **1**, 20-29.

Karis, A., Pata, I., van Doorninck, J. H., Grosveld, F., de Zeeuw, C. I., de Caprona, D. and Fritzsch, B. (2001). Transcription factor GATA-3 alters pathway selection of olivocochlear neurons and affects morphogenesis of the ear. *J. Comp. Neurol.* **429**, 615-630.

Kennedy, T. E., Serafini, T., la Torre de, S., Jr and Tessier-Lavigne, M. (1994). Netrins are diffusible chemotropic factors for commissural axons in the embryonic spinal cord. *Cell* **78**, 425-435.

Kidd, T., Bland, K. S. and Goodman, C. S. (1999). Slit is the midline repellent for the robo receptor in Drosophila. *Cell* **96**, 785-794.

Kitsukawa, T., Shimizu, M., Sanbo, M., Hirata, T., Taniguchi, M., Bekku, Y., Yagi, T. and Fujisawa, H. (1997). Neuropilin-semaphorin III/D-mediated chemorepulsive signals play a crucial role in peripheral nerve projection in mice. *Neuron* **19**, 995-1005.

Long, H., Sabatier, C., Ma, L., Plump, A., Yuan, W., Ornitz, D. M., Tamada, A., Murakami, F., Goodman, C. S. and Tessier-Lavigne, M. (2004). Conserved roles for Slit and Robo proteins in midline commissural axon guidance. *Neuron* **42**, 213-223.

Mombaerts, P., Wang, F., Dulac, C., Chao, S. K., Nemes, A., Mendelsohn, M., Edmondsen, J. and Axel, R. (1996). Visualizing an olfactory sensory map. *Cell* **87**, 675-686.

Momose, T., Tonegawa, A., Takeuchi, J., Ogawa, H., Umesono, K. and Yasuda, K. (1999). Efficient targeting of gene expression in chick embryos by microelectroporation. *Dev. Growth Differ.* **41**, 335-344.

Mueller, B. K. (1999). Growth cone guidance: first steps towards a deeper understanding. *Annu. Rev. Neurosci.* **22**, 351-388.

Naeem, A., Abbas, L. and Guthrie, S. (2002). Comparison of the effects of HGF, BDNF, CT-1, CNTF, and the branchial arches on the growth of embryonic cranial motor neurons. *J. Neurobiol.* **51**, 101-114.

Nguyen Ba-Charvet, K. T., Brose, K., Marillat, V., Kidd, T., Goodman, C. S., Tessier-Lavigne, M., Sotelo, C. and Chedotal, A. (1999). Slit2-mediated chemorepulsion and collapse of developing forebrain axons. *Neuron* **22**, 463-473.

Patel, K., Nash, J. A., Itoh, A., Liu, Z., Sundaresan, V. and Pini, A. (2001). Slit proteins are not dominant chemorepellents for olfactory tract and spinal motor axons. *Development* **128**, 5031-5037.

Pattyn, A., Vallstedt, A., Dias, J. M., Sander, M. and Ericson, J. (2003). Complementary roles for Nkx6 and Nkx2 class proteins in the establishment of motoneuron identity in the hindbrain. *Development* **130**, 4149-4159.

Plump, A. S., Erskine, L., Sabatier, C., Brose, K., Epstein, C. J., Goodman, C. S., Mason, C. A. and Tessier-Lavigne, M. (2002). Slit1 and Slit2 cooperate to prevent premature midline crossing of retinal axons in the mouse visual system. *Neuron* **33**, 219-232.

Rajagopalan, S., Nicolas, E., Vivancos, V., Berger, J. and Dickson, B. J. (2000). Crossing the midline: roles and regulation of Robo receptors. *Neuron* **28**, 767-777.

Serafini, T., Colamarino, S. A., Leonardo, E. D., Wang, H., Beddington, R., Skarnes, W. C. and Tessier-Lavigne, M. (1996). Netrin-1 is required for commissural axon guidance in the developing vertebrate nervous system. *Cell* **87**, 1001-1014.

Shu, T., Sundaresan, V., McCarthy, M. M. and Richards, L. J. (2002). Slit2 guides both precrossing and postcrossing callosal axons at the midline in vivo. *J. Neurosci.* **23**, 8176-8184.

Simmons, D. D. (2002). Development of the inner ear efferent system across vertebrate species. *J. Neurobiol.* **53**, 228-250.

Simon, H. and Lumsden, A. (1993). Rhombomere-specific origin of the contralateral vestibulo-acoustic efferent neurons and their migration across the embryonic midline. *Neuron* **11**, 209-220.

Simon, H., Guthrie, S. and Lumsden, A. (1994). Regulation of SC1/DM-GRASP during the migration of motor neurons in the chick embryo brain stem. *J. Neurobiol.* **25**, 1129-1143.

Simpson, J. H., Kidd, T., Bland, K. S and Goodman, C. S. (2000). Short-range and long-range guidance by Slit and its Robo receptors: Robo and Robo2 play distinct roles in midline guidance. *Neuron* **28**, 753-766.

Stein, E. and Tessier-Lavigne, M. (2001). Hierarchical organization of guidance receptors: silencing of netrin attraction by slit through a Robo/DCC receptor complex. *Science* **291**, 1928-1938.

Studer, M., Ariza-McNaughton, L., Bradley, A. and Krumlauf, R. (1996). Altered segmental identity and abnormal migration of motor neurons in mice lacking Hoxb-1. *Nature* **384**, 630-634.

Sundaresan, V., Mambitisaeva, E., Andrews, W., Annan, A., Knoll, B., Tear, G. and Bannister, L. (2004). Dynamic expression patterns of Robo (Robo1 and Robo2 in the developing murine central nervous system. *J. Comp. Neurol.* **468**, 467-481.

Taniguchi, M., Yuasa, S., Fujisawa, H., Naruse, I., Saga, S., Mishina, M. and Yagi, T. (1997). Disruption of semaphorin III/D gene causes severe abnormality in peripheral nerve projection. *Neuron* **19**, 519-530.

Vallstedt, A., Muhr, J., Pattyn, A., Pierani, A., Mendelsohn, M., Sander, M., Jessell, T. M. and Ericson, J. (2001). Different levels of repressor

activity assign redundant and specific roles to Nkx genes in motor neuron and interneuron specification. *Neuron* **31**, 743-755.

Varela-Echavarria, A., Pfaff, S. L. and Guthrie, S. (1996). Differential expression of LIM homeobox genes among motor neuron subpopulations in the developing chick brain stem. *Mol. Cell Neurosci.* **8**, 242-257.

Varela-Echavarria, A., Tucker, A., Puschel, A. W. and Guthrie, S. (1997). Motor axon subpopulations respond differentially to the chemorepellents netrin-1 and semaphorin D. *Neuron* **18**, 193-207.

Warrilow, J. and Guthrie, S. (1999). Rhombomere origin plays a role in the specificity of cranial motor axon projections in the chick. *Eur. J. Neurosci.* **11**, 1403-1413.

Whitford, K. L., Marillat, V., Stein, E., Goodman, C. S., Tessier-Lavigne, M., Chedotal, A. and Ghosh, A. (2002). Regulation of cortical dendrite development by Slit-Robo interactions. *Neuron* **33**, 47-61.

Yuan, W., Zhou, L., Chen, J. H., Wu, J. Y., Rao, Y. and Ornitz, D. M. (1999). The mouse SLIT family: secreted ligands for ROBO expressed in patterns that suggest a role in morphogenesis and axon guidance. *Dev. Biol.* **212**, 290-306.

Zou, Y., Stoeckli, E., Chen, H. and Tessier-Lavigne, M. (2000). Squeezing axons out of the gray matter: a role for slit and semaphorin proteins from midline and ventral spinal cord. *Cell* **102**, 363-371.